

Self-similar propagation of optical pulses in fibers with positive quartic dispersion

ANTOINE F. J. RUNGE^{1,*}, TRISTRAM J. ALEXANDER¹, JOSEPH NEWTON¹, PRANAV A. ALAVANDI¹, DARREN D. HUDSON², ANDREA BLANCO-REDONDO³, AND C. MARTIJN DE STERKE^{1,4}

¹Institute of Photonics and Optical Science (IPOS), School of Physics, The University of Sydney, NSW 2006, Australia

²CACI Photonics Solutions, 15 Vreeland Road, Florham Park, NJ 07932, USA

³Nokia Bell Labs, 791 Holmdel Road, Holmdel, NJ 07733, USA

⁴The University of Sydney Nano Institute (Sydney Nano), The University of Sydney, NSW 2006, Australia

*Corresponding author: antoine.runge@sydney.edu.au

Compiled September 4, 2022

We study the propagation of ultrashort pulses in optical fiber with gain and positive (or normal) quartic dispersion by self-similarity analysis of the modified nonlinear Schrödinger equation. We find an exact asymptotic solution, corresponding to a triangle-like, $T^{4/3}$ intensity profile, with a $T^{1/3}$ chirp, which is confirmed by numerical simulations. This solution follows different amplitude and width scaling compared to the conventional case with quadratic dispersion. We also suggest, and numerically investigate, a fiber laser consisting of components with positive quartic dispersion which emits quartic self-similar pulses. © 2022 Optical Society of America

<http://dx.doi.org/10.1364/ao.XX.XXXXXX>

Ultrashort optical pulses have played a central role in many breakthrough photonics applications [1, 2]. In the normal dispersion regime ($\beta_2 > 0$), bright solitonic pulses do not exist, but in the presence of gain, input pulses evolve toward pulses with parabolic intensity profiles [3, 4]. Detailed analysis based on self-similarity methods showed that these parabolic pulses are exact asymptotic solutions of the nonlinear Schrödinger equation (NLSE), and propagate self-similarly in optical amplifiers, with exponential scaling of the amplitude and temporal width [5, 6]. This solution displays outstanding robustness against perturbations and allows for the generation of high-energy pulses [7, 8]. These pulses possess a linear chirp which means that they can be recompressed to generate ultrashort pulses with high peak powers. These remarkable properties have been at the basis of a new generation of fiber amplifiers [9] and lasers [10].

So far, studies have focused on waveguides with second-order dispersion, as it usually is the dominant contribution. There have been investigations of nonlinear pulse propagation in the presence of second- and fourth-order dispersion. Most relevant is the numerical study of Bale *et al.*, who reported the formation of triangular pulses and of pulses with double-peaked spectra [11]. In addition to this, recent work shows optical pulses arising from the interaction of only negative fourth-order disper-

sion ($\beta_4 < 0$) and the Kerr nonlinearity [12]. These pure-quartic solitons have novel, interesting properties and have stimulated theoretical research [13, 14], and the development of laser systems with dominant quartic dispersion [15, 16]. Given the similar physics of conventional and pure-quartic solitons, one might ask whether optical pulses also propagate self-similarly in the presence of gain and positive quartic dispersion.

In this Letter, we theoretically and numerically study the self-similar propagation of optical pulses in a medium with positive fourth-order dispersion (i.e., $\beta_4 > 0$) and distributed gain. We find that the pulses evolve toward a new asymptotic solution with temporal and spectral profiles that differ significantly from the quadratic dispersion case. After this we simulate the pulse evolution in a laser cavity design consisting of components with positive quartic dispersion. Our results show that, similarly to parabolic pulses [10, 17] and all-normal dispersion lasers [18], the addition of a spectral filter to compensate for the accumulated chirp leads to a laser that emits quartic self-similar pulses. We expect our results to stimulate follow-up investigations of pulse dynamics in systems with complicated dispersion profiles, in areas as diverse as laser physics and applied mathematics.

We begin our analysis by considering the propagation of an optical pulse in a quartic dispersion medium with distributed gain. In the absence of gain saturation and for pulses with spectral bandwidths narrower than the amplification bandwidth, this evolution can be described by the modified NLSE

$$i \frac{\partial \psi}{\partial z} = \frac{\beta_4}{4!} \frac{\partial^4 \psi}{\partial T^4} - \gamma \psi |\psi|^2 + i \frac{g}{2} \psi, \quad (1)$$

where $\psi = \psi(z, T)$ is the slowly varying amplitude of the pulse's envelope with respect to a carrier frequency ω_0 , z is the propagation coordinate, β_4 is the fourth-order dispersion, T is the pulse local time, γ is the nonlinear parameter and g is the distributed gain coefficient. The evolution of the pulse energy $E_p(z) = \int_{-\infty}^{\infty} |\psi(z, T)|^2 dT$ in the amplifier must satisfy the conservation integral

$$E_p(z) = E_p(0) e^{gz}. \quad (2)$$

In the presence of quadratic dispersion, the width of self-similar pulses increases as $e^{gz/3}$, whereas their power scales as $e^{2gz/3}$, consistent with Eq. (2).

To find a self-similar solution in the presence of quartic dispersion, we look for a solution with a positive definite amplitude and phase of the form $\psi(z, T) = A(z, T)e^{i\varphi(z, T)}$. By substituting this into Eq. (1) we find a complex equation, the real and imaginary parts of which can be written separately. Each of these equations has many terms stemming from the fourth partial time derivative. As discussed later, the asymptotic terms, the terms that dominate as $z \rightarrow \infty$, are those with the highest powers of φ and its time derivatives, giving

$$A_z - \frac{g}{2}A = \frac{\beta_4}{12} \left(2A_T(\varphi_T)^3 + 3A(\varphi_T)^2\varphi_{TT} \right), \quad (3)$$

$$\varphi_z = \frac{\beta_4}{24}(\varphi_T)^4 - \gamma A^2, \quad (4)$$

where the subscripts indicate partial derivatives.

Equations (3) and (4) can be solved in closed form provided that $\gamma\beta_4 > 0$, and give

$$A(z, T) = A_0 e^{2gz/7} \left[1 - \left(\frac{T}{T_0(z)} \right)^{4/3} \right]^{1/2}, \quad (5)$$

where

$$A_0 = \left(\frac{3E_{in}}{16} \right)^{2/7} \left(\frac{3g^4}{2\beta_4\gamma^3} \right)^{1/14} \quad (6)$$

$$T_0(z) = 7 \left(\frac{2}{3} \right)^{5/4} \left(\frac{\beta_4^{1/4}(\gamma A_0^2)^{3/4}}{g} \right) e^{3gz/7}, \quad (7)$$

where E_{in} is the input pulse energy. Solution (5) is valid for $|T| \leq T_0(z)$; for $|T| > T_0(z)$, $A(z, T) = 0$. The temporal phase is

$$\varphi(z, T) = \varphi_0 - \frac{3}{2} \left(\frac{9g}{28\beta_4} \right)^{1/3} T^{4/3} + \frac{7}{4g} \gamma A_0^2 e^{4gz/7}, \quad (8)$$

with φ_0 an arbitrary constant. This corresponds to an instantaneous frequency $\delta\omega(T) = -\partial\varphi(z, T)/\partial T = 2(9g/28\beta_4)^{1/3} T^{1/3}$.

Equations (5)-(8) show that in the asymptotic regime the pulse maintains its shape, with the intensity having a $(1 - (T/T_0))^{4/3}$ dependence, and the instantaneous frequency having a $T^{1/3}$ chirp. They further show that both the width and the intensity grow exponentially, with a fraction 3/7 of the total gain used to increase the pulse width and a fraction 4/7 used to increase the pulse intensity. Hence the total pulse energy increases as $\exp(gz)$ consistent with Eq. (2) [8].

The time dependence of the self-similar pulses can be understood using an extension of the argument of Anderson *et al.* [3]. When a pulse propagates through a Kerr nonlinear medium, it generates new frequency components, that are shifted by an amount proportional to $\delta\omega_{NL} \propto -\partial I/\partial t$ [19], so red-shifted frequencies appear on the pulse's leading edge and blue-shifted frequencies appear on its trailing edge. For the self-similar pulses, Eq. (5) shows that $\delta\omega_{NL} \propto T^{1/3}$, and so the nonlinearly generated frequencies align with the instantaneous frequency that also varies as $T^{1/3}$. This consistency has the following consequence: in the presence of quartic dispersion the group velocity varies approximately as $(\Delta\omega)^3$ about ω_0 . The $T^{1/3}$ instantaneous frequency, implies that $T \propto (\Delta\omega)^3$, so the local group velocity depends linearly on T . The effect of this is that the pulse maintains the $T^{1/3}$ instantaneous frequency, and grows uniformly without wave breaking [3]. At a more general level, this argument shows that the essence of the self-similar pulse is its chirp, and that the intensity adjusts to maintain this chirp.

To confirm these theoretical predictions, we performed a set of numerical simulations of Eq. (1) using a standard split-step Fourier method [19]. We used Gaussian input pulses with pulse durations (FWHM) ranging from 250 fs – 1 ps but with fixed input energy $E_{in} = 15$ pJ, in a 7 m long fiber amplifier. The fiber parameters are: quartic dispersion $\beta_4 = +1$ ps⁴/km; $g = 1.9$ m⁻¹; $\gamma = 5.8$ W⁻¹km⁻¹. The values of g and γ are typical for single-mode Yb-doped fibers [5, 6]. For a pulse duration $T_0 = 200$ fs, the quadratic dispersion coefficient in Ref. [5] ($\beta_2 = +25$ ps²/km) leads to a dispersion length $L_D = T_0^2/\beta_2 = 1.6$ m. To use a similar metric, we chose a quartic dispersion coefficient leading to the same dispersion length so that $\beta_4 = T_0^4/L_D = +1$ ps⁴/km. The quadratic and cubic dispersion coefficients are set to zero in our simulations.

Results of these simulations are summarized in Fig. 1(a), which shows intensity and instantaneous frequency versus time on a linear scale. The inset shows the intensity on a logarithmic scale. Note the excellent agreement between simulations and the asymptotic analytic results Eq. (5)-Eq. (8).

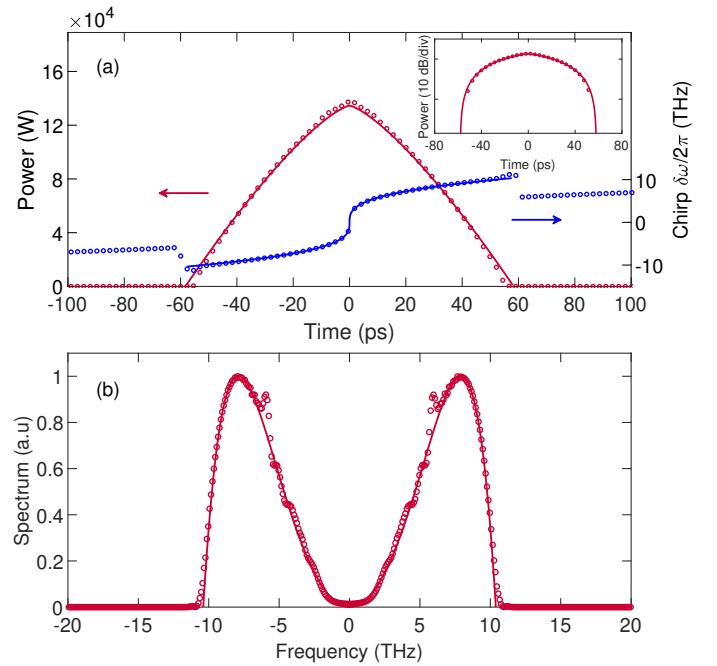


Fig. 1. (a) Simulated output temporal intensity (red circles, left axis) and chirp (blue circles, right axis) for a 15 pJ, 250 fs FWHM Gaussian input pulse, compared to the asymptotic intensity and instantaneous phase following from Eqs (5)-(8) (solid curves). Inset: intensity profile and asymptotic solution on logarithmic scale. (b) Corresponding simulated (red circles) and asymptotic (solid red line) spectra.

Using the method of stationary phase it is possible to find an approximate analytical expression for the pulse spectrum [3, 8, 20]. It is also self-similar, and takes the form

$$|F(\omega)|^2 \propto A_0^2 \left(\omega^2 e^{4gz/7} - K\omega^6 \right), \quad (9)$$

where $K = \beta_4/(24\gamma A_0^2)$, and negative values of the right-hand side are to be taken to be zero. Thus the spectrum is double-peaked, with a total width equal to $2K^{1/4}e^{gz/7}$, and a peak amplitude that scales with $e^{6gz/7}$, so that the total energy scales as e^{8gz} , as required. In contrast, in the presence of quadratic dispersion

the spectrum is parabolic with the gain distributed 1/3 : 2/3 between the spectral width and peak intensity, respectively.

Associated simulation results in Fig. 1(b) are in excellent agreement with Eq. (9). Considering the entire Fig. 1, we understand the double-peaked spectrum. The strong temporal chirp at $T = 0$ (Fig. 1(a)), causes the pulse's leading and trailing halves to have different frequencies. Because the dispersion is positive, the front half of the pulse corresponds to the low-frequency lobe, whereas the back half of the pulse corresponds to the high-frequency lobe. This is confirmed in Fig. 2 which shows the temporal intensities of the spectrally filtered simulated pulse (see inset). **We note that the time and spectral shapes in Figs 1 are reminiscent of the results of Bale *et al* [11].**

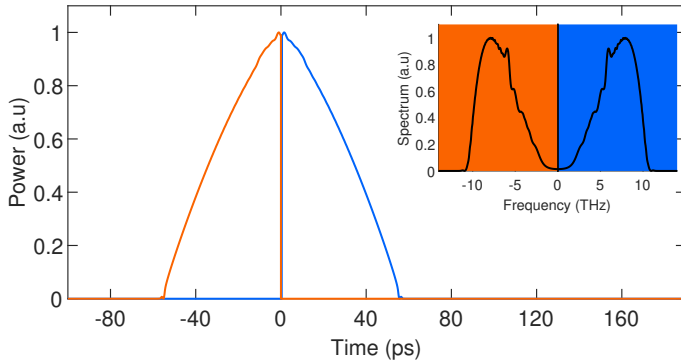


Fig. 2. Filtered temporal intensity profiles corresponding to the low-frequency (orange) and high-frequency (blue) lobes. Inset shows the corresponding filtered spectra.

One of the implications of Eq. (6) is that the asymptotic pulse evolution only depends on the energy of the initial pulse and not on its shape or duration, consistent with the case of quadratic dispersion [5, 8]. In order to test this, and to examine how pulses evolve throughout the fiber, we refer to Fig. 3 in which we compare the evolution of (a) the amplitude, and, (b), the pulse width with the analytic prediction for $A(z, T)$ and $T_0(z, T)$ in Eq. (6) and Eq. (7), respectively. In all cases the simulations converge to the same asymptotic solution. For a given input pulse, the asymptotic limit is reached in a shorter propagation distance as the fiber gain is increased, consistent with observations for quadratic dispersion [5]. We carried out additional simulations (not shown here) to confirm that our conclusions do not depend on the fiber parameters.

From the full pulse evolution in Fig. 3 we note that for the longer pulses, the pulse width is initially approximately constant. This is because these pulse are too weak for significant nonlinear effects, and the dispersion-induced chirp is not sufficiently large to lead to pulse broadening. Hence, at this early stage the pulse's power grows as $e^{\beta z}$, but its intensity is otherwise unchanged. This evolution then enters a more complicated phase where both the dispersion and the nonlinearity act, until, in the asymptotic regime, the evolution again simplifies and only the terms in Eq. (3) and Eq. (4) contribute significantly.

Having investigated the self-similar solutions in an ideal longitudinally invariant environment, we consider the generation of such pulses in a fiber laser. A conceptual model for this laser is shown in Fig. 4(a). It is similar to the geometry considered by Ilday *et al.* [10], except that the fibre in the cavity has (positive) quartic dispersion. The laser contains a 7 m segment of passive quartic fiber (PQF) and 1 m of doped quartic fiber. Both fibers are considered to be single-mode with dispersion and nonlinear

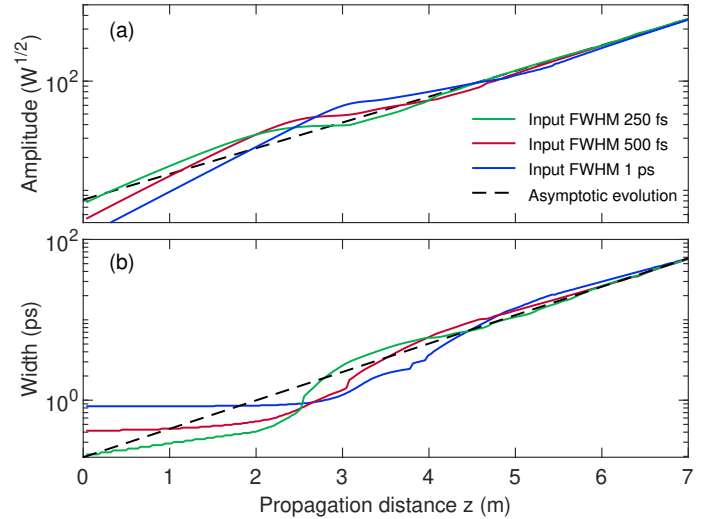


Fig. 3. Evolution of (a) the amplitude; and (b) the width versus propagation distance for 15 pJ Gaussian pulses with three different pulse widths: 0.25 ps (green), 0.5 ps (red), and 1 ps (blue). The prediction from the asymptotic solution is indicated by the dashed black line.

parameters similar to the simulations described above. **The gain in the doped-fiber is calculated using $g = g_0 / (1 + E(z) / E_{sat})$, where g_0 is the small-signal gain corresponding to 30 dB, $E(z)$ is the pulse energy and E_{sat} is the saturation energy [10].** The mode-locking element is a saturable absorber (SA) modelled by a transfer function $T = 1 - q_0 / (1 + P(T) / P_{sat})$, where $q_0 = 0.7$ is the unsaturated loss, $P(T)$ is the instantaneous pulse power and P_{sat} is the saturation power [10]. An output coupler (OC) is located after the SA which extracts 50% of the intracavity power. At the end of each roundtrip, a bandpass spectral filter (15 nm bandwidth) clips the pulse to compensate for the accumulated chirp and to reset the electric field before the next roundtrip.

The propagation in the PQF and in the doped fiber is simulated with the split-step Fourier method as above, and the initial field is Gaussian random noise multiplied by a sech shape in the time domain. The temporal intensity, instantaneous frequency and the spectrum of a typical output pulse for $\beta_4 L = 0.008 \text{ ps}^4$, $P_{sat} = 1 \text{ kW}$, and $E_{sat} = 30 \text{ nJ}$ are shown in Fig. 4(b) and (c). The temporal intensity of the pulse at the laser output (red solid curve), which has a pulse energy of 7 nJ, matches Eq. (5) quite well (dashed blue curve), except at low intensity levels. The instantaneous frequency (solid green curve) similarly matches the analytic result (dashed dark red curve) Eq. (8). Figure 4(c) shows the associated spectrum. The result of the laser simulation again matches analytic result Eq. (9) well. The agreement in this case is not as good as in Figs. 1 because the laser, consisting of lumped elements, is a non-ideal environment. In particular, in this configuration, the OC is located after the SA which follows a power-dependent transmission function, modifying slightly the shape of the spectrum. Nonetheless, overall the laser output matches the analytic results well.

Now that we ascertained that the asymptotic solutions match the numerical results, we discuss why the time-derivative terms in Eq. (3) and Eq. (4) are the asymptotic ones. The terms that were dropped contain lower powers of φ , but involve higher time derivatives. Since $\delta\omega \propto T^{1/3}$, high time derivatives vanish when $|T|$ is sufficiently large, with the highest derivatives vanishing fastest. Therefore, sufficiently far from the centre of the

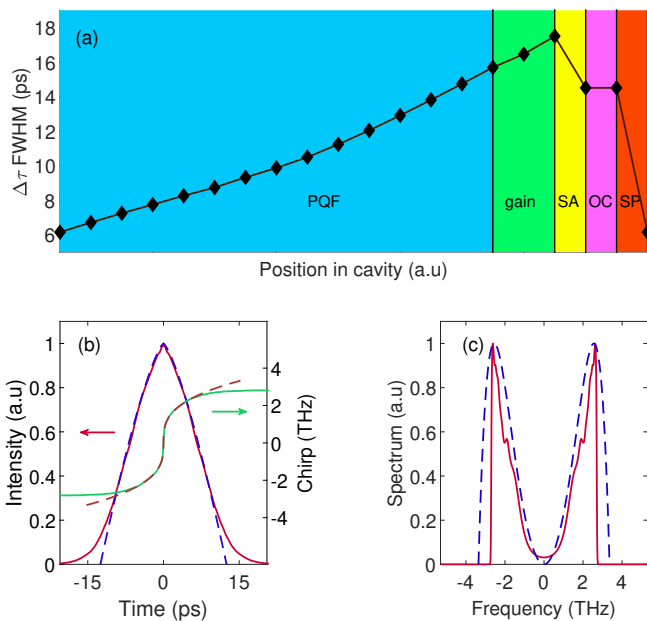


Fig. 4. (a) Schematic of the simulated laser cavity. POF: passive quartic fiber; SA: saturable absorber; OC: output coupler; SP: Spectral filter. Black diamonds indicate the evolution of the pulse's FWHM over a cavity round trip. (b) Emitted temporal intensity (red curve, left axis) and instantaneous frequency (green curve, right axis). (c) Corresponding output spectrum. Dashed curve indicates asymptotic fit calculated from Eqs. (5), (8) and (9).

pulse, these terms are negligible. In practice, these terms only contribute for $|T| \lesssim (\beta_4/g)^{1/4} \approx 100$ fs for our parameters, and thus they are increasingly irrelevant as the pulse propagates.

We have considered the gain to be dispersionless, even though the bandwidth in Fig. 1(b) is approximately 20 THz, corresponding to 70 nm at $\lambda \approx 1 \mu\text{m}$. This is less than in previous work for quadratic dispersion, in which experiments and theory matched well [5]. However, gain dispersion eventually causes discrepancies requiring a more complete model [21].

Potential applications of the self-similar pulses investigated here stem from their temporal and spectral shapes. The strong chirp causes the double-peaked spectrum, which may have applications in two-color spectroscopy or for generating wavelength-multiplexing structures [22]. These pulses could also be used for terahertz or far-infrared generation via difference frequency mixing [23]. The pulses have a $T^{1/3}$ instantaneous frequency, which is more difficult to compensate than the linear instantaneous frequency (linear chirp) that arises for self-similar pulses in a quadratically dispersive medium.

As a final comment, note that analytic expressions (5) and (9) imply finite support in both time and frequency, which contradicts the Amrein-Berthier theorem [24]. However since these expressions are approximate there is no contradiction—when exact numerical solutions are considered it is found that the theorem is not violated.

In conclusion, we have studied theoretically and numerically the self-similar propagation of optical pulses in the presence of positive quartic dispersion, Kerr nonlinearity and gain. We found an exact asymptotic solution, corresponding to a pulse with a $T^{4/3}$ temporal intensity profile, and a $T^{1/3}$ chirp. This

large, steep chirp gives rise to a double-peaked spectrum. We also showed that by using a laser architecture similar to a positive dispersion cavity [10, 17] to compensate for the large accumulated chirp, fiber lasers emitting quartic self-similar pulses can be achieved. As optical fibers with dominant positive quartic dispersion are not currently available, an alternative approach based on the tailoring of the net-cavity dispersion could be used to generate these new self-similar pulses [16].

FUNDING

Australian Research Council (ARC) Discovery Project (DP180102234); Asian Office of Aerospace R&D (AOARD) grant (FA2386-19-1-4067).

ACKNOWLEDGMENT

The authors thank Prof. John. D. Harvey from the University of Auckland and Dr. Dane Austin from Fathom Computing for fruitful discussions and suggestions.

DISCLOSURE

The authors declare no conflicts of interest.

REFERENCES

1. S. Diddams, L. Hollberg, and V. Mbele, *Nature* **445**, 627 (2007).
2. J. M. Dudley, G. Genty, and S. Coen, *Rev. Mod. Phys.* **78**, 1135 (2006).
3. D. Anderson, M. Desaix, M. Karlsson, M. Lisak, and M. L. Quiroga-Teixeiro, *J. Opt. Soc. Am. B* **10**, 1185 (1993).
4. K. Tamura and M. Nakazawa, *Opt. Lett.* **21**, 68 (1996).
5. M. E. Fermann, V. I. Kruglov, B. C. Thomsen, J. M. Dudley, and J. D. Harvey, *Phys. Rev. Lett.* **84**, 6010 (2000).
6. J. M. Dudley, C. Finot, D. J. Richardson, and G. Millot, *Nat. Phys.* **3**, 597–603 (2007).
7. V. I. Kruglov, A. C. Peacock, J. M. Dudley, and J. D. Harvey, *Opt. Lett.* **25**, 1753 (2000).
8. V. I. Kruglov, A. C. Peacock, J. D. Harvey, and J. M. Dudley, *J. Opt. Soc. Am. B* **19**, 461 (2002).
9. J. Limpert, T. Schreiber, T. Clausnitzer, K. Zöllner, H.-J. Fuchs, E.-B. Kley, H. Zellmer, and A. Tünnermann, *Opt. Express* **10**, 628 (2002).
10. F. Ilday, J. R. Buckley, W. G. Clark, and F. W. Wise, *Phys. Rev. Lett.* **92**, 213902 (2004).
11. B. G. Bale, S. Boscolo, K. Hammani, and C. Finot, *J. Opt. Soc. Am. B* **28**, 2059 (2011).
12. A. Blanco-Redondo, C. M. de Sterke, J. E. Sipe, T. F. Krauss, B. J. Eggleton, and C. Husko, *Nat. Comm.* **7**, 10427 (2016).
13. K. K. K. Tam, T. J. Alexander, A. Blanco-Redondo, and C. M. de Sterke, *Opt. Lett.* **44**, 3306 (2019).
14. H. Taheri and A. B. Matsko, *Opt. Lett.* **44**, 3086 (2019).
15. C. W. Lo, A. Stefani, C. M. de Sterke, and A. Blanco-Redondo, *Opt. Express* **26**, 7786 (2018).
16. A. F. J. Runge, D. D. Hudson, K. K. K. Tam, C. M. de Sterke, and A. Blanco-Redondo, *Nat. Photonics* (2020).
17. W. H. Renninger, A. Chong, and F. W. Wise, *Phys. Rev. A* **82**, 021805 (2010).
18. A. Chong, J. Buckley, W. Renninger, and F. Wise, *Opt. Express* **21**, 10095 (2006).
19. G. P. Agrawal, *Nonlinear fibre Optics* (Academic Press, 1995), 2nd ed.
20. F. W. J. Olver, *Asymptotics and Special Functions* (Academic Press, 1974), 1st ed.
21. A. C. Peacock, R. J. Kruhlak, J. D. Harvey, and J. M. Dudley, *Opt. Comm.* **206**, 171 (2002).
22. N. Verschueren and C. Finot, *Electron. Lett.* **47**, 1194 (2011).
23. Y. J. Ding, *J. Opt. Soc. Am. B* **31**, 2696 (2014).
24. M. Hill, "The uncertainty principle for fourier transforms on the real line," (2013).

FULL REFERENCES

1. S. Diddams, L. Hollberg, and V. Mbele, "Molecular fingerprinting with the resolved modes of a femtosecond laser frequency comb," *Nature* **445**, 627–630 (2007).
2. J. M. Dudley, G. Genty, and S. Coen, "Supercontinuum generation in photonic crystal fiber," *Rev. Mod. Phys.* **78**, 1135–1184 (2006).
3. D. Anderson, M. Desaix, M. Karlsson, M. Lisak, and M. L. Quiroga-Teixeiro, "Wave-breaking-free pulses in nonlinear-optical fibers," *J. Opt. Soc. Am. B* **10**, 1185–1190 (1993).
4. K. Tamura and M. Nakazawa, "Pulse compression by nonlinear pulse evolution with reduced optical wave breaking in erbium-doped fiber amplifiers," *Opt. Lett.* **21**, 68–70 (1996).
5. M. E. Fermann, V. I. Kruglov, B. C. Thomsen, J. M. Dudley, and J. D. Harvey, "Self-similar propagation and amplification of parabolic pulses in optical fibers," *Phys. Rev. Lett.* **84**, 6010 (2000).
6. J. M. Dudley, C. Finot, D. J. Richardson, and G. Millot, "Self-similarity in ultrafast nonlinear optics," *Nat. Phys.* **3**, 597–603 (2007).
7. V. I. Kruglov, A. C. Peacock, J. M. Dudley, and J. D. Harvey, "Self-similar propagation of high-power parabolic pulses in optical fiber amplifiers," *Opt. Lett.* **25**, 1753–1755 (2000).
8. V. I. Kruglov, A. C. Peacock, J. D. Harvey, and J. M. Dudley, "Self-similar propagation of parabolic pulses in normal-dispersion fiber amplifiers," *J. Opt. Soc. Am. B* **19**, 461–469 (2002).
9. J. Limpert, T. Schreiber, T. Clausnitzer, K. Zöllner, H.-J. Fuchs, E.-B. Kley, H. Zellmer, and A. Tünnermann, "High-power femtosecond yb-doped fiber amplifier," *Opt. Express* **10**, 628–638 (2002).
10. F. Ilday, J. R. Buckley, W. G. Clark, and F. W. Wise, "Self-similar evolution of parabolic pulses in a laser," *Phys. Rev. Lett.* **92**, 213902 (2004).
11. B. G. Bale, S. Boscolo, K. Hammani, and C. Finot, "Effects of fourth-order fiber dispersion on ultrashort parabolic optical pulses in the normal dispersion regime," *J. Opt. Soc. Am. B* **28**, 2059–2065 (2011).
12. A. Blanco-Redondo, C. M. de Sterke, J. E. Sipe, T. F. Krauss, B. J. Eggleton, and C. Husko, "Pure-quartic solitons," *Nat. Comm.* **7**, 10427 (2016).
13. K. K. K. Tam, T. J. Alexander, A. Blanco-Redondo, and C. M. de Sterke, "Stationary and dynamical properties of pure-quartic solitons," *Opt. Lett.* **44**, 3306–3309 (2019).
14. H. Taheri and A. B. Matsko, "Quartic dissipative solitons in optical kerr cavities," *Opt. Lett.* **44**, 3086–3089 (2019).
15. C. W. Lo, A. Stefani, C. M. de Sterke, and A. Blanco-Redondo, "Analysis and design of fibers for pure-quartic solitons," *Opt. Express* **26**, 7786–7796 (2018).
16. A. F. J. Runge, D. D. Hudson, K. K. K. Tam, C. M. de Sterke, and A. Blanco-Redondo, "The pure-quartic soliton laser," *Nat. Photonics* (2020).
17. W. H. Renninger, A. Chong, and F. W. Wise, "Self-similar pulse evolution in an all-normal-dispersion laser," *Phys. Rev. A* **82**, 021805 (2010).
18. A. Chong, J. Buckley, W. Renninger, and F. Wise, "All-normal-dispersion femtosecond fiber laser," *Opt. Express* **21**, 10095–10100 (2006).
19. G. P. Agrawal, *Nonlinear fibre Optics* (Academic Press, 1995), 2nd ed.
20. F. W. J. Olver, *Asymptotics and Special Functions* (Academic Press, 1974), 1st ed.
21. A. C. Peacock, R. J. Kruhlak, J. D. Harvey, and J. M. Dudley, "Solitary pulse propagation in high gain optical fiber amplifiers with normal group velocity dispersion," *Opt. Comm.* **206**, 171–177 (2002).
22. N. Verschueren and C. Finot, "Pulse doubling and wavelength conversion through triangular nonlinear pulse reshaping," *Electron. Lett.* **47**, 1194–1196 (2011).
23. Y. J. Ding, "Progress in terahertz sources based on difference-frequency generation," *J. Opt. Soc. Am. B* **31**, 2696–2711 (2014).
24. M. Hill, "The uncertainty principle for fourier transforms on the real line," (2013).